

1 **Atmospheric predictability: the origins of the finite-time behaviour**

2 Tsz Yan Leung*

3 *Department of Mathematics and Statistics, University of Reading, United Kingdom*

4 Martin Leutbecher

5 *European Centre for Medium-range Weather Forecasts, Reading, United Kingdom*

6 Sebastian Reich

7 *Institute of Mathematics, University of Potsdam, Germany*

8 Theodore G. Shepherd

9 *Department of Meteorology, University of Reading, United Kingdom*

10 *Corresponding author address: Department of Mathematics and Statistics, Whiteknights, PO Box

11 220, Reading RG6 6AX, United Kingdom

12 E-mail: tsz.leung@pgr.reading.ac.uk

ABSTRACT

13 First proposed by Edward N. Lorenz in 1969, the existence of a finite-time
14 barrier in deterministically predicting atmospheric flows is now well-accepted
15 in the community of dynamical meteorology. The present work argues via nu-
16 merical simulation that Lorenz's model may be over-simplified. The apparent
17 contradiction between a finite-time barrier to predictability and the proof of
18 well-posedness of the incompressible two-dimensional Navier-Stokes equa-
19 tions, regardless of the slope of the kinetic energy spectrum, is reconciled
20 through understanding of this slope's practical role in a particular error bound
21 of the analytic proof.

22 1. Introduction

23 Now an accepted fact in dynamical meteorology, the existence of a finite-time barrier in deter-
24 ministically predicting atmospheric flows was first conceptually shown by Lorenz (1969). In his
25 seminal paper, he made the distinction between fluid systems whose error at any future time can
26 be made arbitrarily small by suitably reducing the initial error, and those whose error at any future
27 time cannot be reduced below a certain limit unless the initial error is zero. These systems were
28 characterised in terms of *range of predictability* (or simply *predictability*; the reader is referred
29 to Appendix A for a motivation of the concept): the former category has an infinite range and
30 the latter has only a finite range. By modelling atmospheric flows by the two-dimensional (2D)
31 barotropic vorticity equation and assuming a $-\frac{5}{3}$ exponent in the power-law relationship of the
32 kinetic energy (KE) spectrum (the *spectral slope*, as a power-law in a log-log plot is a straight line
33 with the slope being the exponent) for the unperturbed flow, he argued that such flows have a finite
34 range of predictability.

35 Although the barotropic vorticity equation with large-scale forcing produces a steeper spectral
36 slope of -3 , and unbalanced dynamics are required to produce a spectral slope of $-\frac{5}{3}$ in more
37 realistic models (Sun and Zhang 2016), it has been shown that predictability is determined much
38 more by the spectral slope than by the nature of the dynamics (Rotunno and Snyder 2008). Thus, it
39 is appropriate to use the barotropic vorticity system to study predictability with a range of spectral
40 slopes.

41 Closely related to this system are the incompressible 2D Navier-Stokes (2D-NS) equations,
42 whose well-posedness was first rigorously shown by Ladyzhenskaya also in the second half of
43 the twentieth century (Robinson 2001). As we will see in Section 4, it is not difficult to show that
44 well-posedness implies an infinite range of predictability in the sense of Lorenz.

45 The present paper attempts to bridge the gap between the finite predictability result of Lorenz
 46 and the infinite predictability corollary of Ladyzhenskaya’s proof, in the context of incompressible
 47 2D flows. Section 2 reviews Lorenz’s argument of its finite-time behaviour. In Section 3 we
 48 reproduce Lorenz’s numerical results and discuss the predictability in the directly simulated 2D
 49 barotropic vorticity model. An account of the well-posedness and infinite predictability of the
 50 incompressible 2D-NS equations is presented in Section 4, with which we reconcile Lorenz’s
 51 result of finite predictability in Section 5. The major findings are summarised in Section 6.

52 2. Lorenz’s argument of finite predictability

53 The model of Lorenz (1969) is based on the dimensionless 2D barotropic vorticity equation

$$\frac{\partial \theta}{\partial t} + J(\psi, \theta) = 0, \quad \theta = \Delta \psi \quad (1)$$

54 where ψ is the velocity streamfunction (related to the velocity \mathbf{u} by $\mathbf{u} = -\nabla \times (\psi \hat{\mathbf{k}})$), $\Delta =$
 55 $\nabla \cdot \nabla$, $\nabla = \left(\frac{\partial}{\partial x}, \frac{\partial}{\partial y} \right)$ and $J(A, B) = \frac{\partial A}{\partial x} \frac{\partial B}{\partial y} - \frac{\partial A}{\partial y} \frac{\partial B}{\partial x}$. Assuming a doubly periodic domain, Lorenz
 56 expanded the variables ψ and θ in Fourier series and re-wrote the linearised error equation of
 57 (1) in Fourier components. Then he made various assumptions to an ensemble of error fields
 58 for the linearised error equation of (1), most notably homogeneity and a slight generalisation
 59 of the quasi-normal closure. The resulting equation was then passed into the large-domain and
 60 continuous-spectrum limit.

61 The derivation would have been more straightforward if the domain were the whole \mathbb{R}^2 space and
 62 the variables were Fourier-transformed rather than expanded in Fourier series. We have checked
 63 that this method indeed returns the same equation as the limiting equation of Lorenz, up to a
 64 constant multiplicative factor.

65 A further assumption of isotropy simplifies the equation, which was then discretised and numer-
66 ically approximated. Depending on the specification of a KE spectrum for the unperturbed flow,
67 a matrix of constant coefficients C was constructed so that the vector Z of error KE at different
68 scales (each scale K collectively represents wavenumbers $k = 2^{K-1}$ to $k = 2^K$) evolves according
69 to the linear model

$$\frac{d^2}{dt^2}Z = CZ, \quad \text{or equivalently} \quad \frac{d}{dt} \begin{pmatrix} Z \\ W \end{pmatrix} = \begin{pmatrix} 0 & I \\ C & 0 \end{pmatrix} \begin{pmatrix} Z \\ W \end{pmatrix}. \quad (2)$$

70 As Rotunno and Snyder (2008) mentioned, the computation of C involves computing integrals
71 of nearly singular functions. We have been cautious about these integrations and have made sure
72 that our integrations for C are accurate, some details of which are provided in Appendix B.

73 To time-integrate equation (2), it is necessary that the initial conditions for Z and its first deriva-
74 tive W are specified. Lorenz did not explicitly give an initial condition for W , although it is safe to
75 assume $W(t = 0) \equiv 0$ as was prescribed in the predictability experiments of Rotunno and Snyder
76 (2008). The non-linear effects were accounted for by removing the corresponding components
77 of Z and C when the error KE saturated at a particular scale. Time-integration with the resulting
78 lower-dimensional system was carried on, until all scales became saturated.

79 As Lorenz noted down the saturation times t_K of scale K , he found that the successive differences
80 $t_K - t_{K+1}$ behaved approximately proportional to $2^{-\beta K}$ with β depending on the spectral slope.
81 He therefore concluded that, given an initial error at an infinitesimally small scale, the range of
82 predictability is finite if and only if the telescoping series

$$t_K = \sum_{j=K}^{\infty} (t_j - t_{j+1}) = \sum_{j=K}^{\infty} 2^{-\beta j} \quad (3)$$

83 is summable, which is the case if and only if $\beta > 0$. By observing $\beta = \frac{2}{3}$ for the atmospherically
84 relevant spectral slope of $-\frac{5}{3}$, he concluded finite predictability for the atmosphere. Additionally,

85 he found that $\beta = \frac{1}{3}$ for a hypothetical spectral slope of $-\frac{7}{3}$. Lorenz thus hypothesised by linear
86 extrapolation that the range of predictability would be infinite if the spectral slope were steepened
87 to -3 .

88 **3. Numerical simulations**

89 We performed a series of numerical simulations, first on the Lorenz model (2) followed by a
90 forced-dissipative version of the full 2D barotropic vorticity system (1), to see whether infinite
91 predictability is indeed achieved with a KE spectral slope of -3 as Lorenz hypothesised.

92 *a. Lorenz's model*

93 Rotunno and Snyder (2008) solved for the growth of the error KE spectrum for a background
94 spectral slope of $-p$ where $p = 3$. In order to assess the range of predictability in Lorenz's frame-
95 work, we extended their calculations to study the relationship between K and t_K .

96 Having computed the matrix C as in Rotunno and Snyder (2008), we solved the linear matrix
97 system (2) explicitly, that is, by writing out the general solution in terms of the eigenvalues and
98 eigenvectors of

$$\begin{pmatrix} 0 & I \\ C & 0 \end{pmatrix}$$

99 and projecting the initial condition onto such an eigenspace to determine the constants of the
100 general solution. An advantage of this exact approach to solving the system is that it eliminates
101 the unstable effects brought over by the positive eigenvalues in any numerical scheme, such as
102 those used in Lorenz (1969), Rotunno and Snyder (2008) and its extension by Durran and Gingrich
103 (2014).

104 Figure 1 shows the saturation times t_K as a function of the scale K for the -3 spectrum as in
 105 Rotunno and Snyder (2008), and Figure 2 shows the evolution of the error spectrum. Note that in
 106 Figure 1 t_K is plotted instead of $t_K - t_{K+1}$ against K , but the choice makes little difference when
 107 $\beta > 0$ since if $t_K - t_{K+1}$ is proportional to $2^{-\beta K}$ then so is t_K (cf. equation (3)). It is clear that the
 108 saturation times t_K scale as $2^{-\beta K}$ with a small but positive β (0.05) along the inertial range, so that
 109 the sum in equation (3) is still finite for $p = 3$, contrary to Lorenz’s prediction. Indeed, arguing
 110 in the same way as Lorenz, our result indicates finite predictability for a -3 spectrum which is
 111 contrary to Lorenz’s hypothesis, although we acknowledge that $\beta = 0.05$ is just marginally away
 112 from the critical value of zero.

113 Additionally, we also re-ran Lorenz’s model with background KE spectra of $p = \frac{5}{3}$ and $p = \frac{7}{3}$.
 114 It turned out that the K - t_K relationship is not that straightforward: in some cases it is hard to even
 115 fit a β to the relationship because the graphs look so different to $2^{-\beta K}$. Yet, even with our ‘nicest’
 116 results, the central assumption to Lorenz’s hypothesis (that β varies linearly with p) does not hold:
 117 we found that $\beta = 0.67, 0.27$ for $p = \frac{5}{3}, \frac{7}{3}$ respectively based on our computations. Since we have
 118 no access to his original code, we are unable to explain our divergence with Lorenz who concluded
 119 $\beta = \frac{1}{3}$ for $p = \frac{7}{3}$.

120 *b. Forced-dissipative 2D barotropic vorticity equation*

121 Among the spectral slopes where our values of β differ from Lorenz’s, the -3 spectrum de-
 122 serves particular attention because the difference amounts to a qualitative contrast between finite
 123 and infinite ranges of predictability. To further investigate this, we performed direct numerical
 124 simulations (DNS) on this $p = 3$ spectrum in the form of identical-twin experiments (pairs of
 125 runs which only differ in the initial condition), and assessed the predictability following Lorenz’s
 126 methodology with necessary adaptations.

127 First of all, equation (1) had to be restricted to a doubly periodic domain and be made forced-
 128 dissipative:

$$\frac{\partial \theta}{\partial t} + J(\psi, \theta) = f + d, \quad \theta = \Delta \psi. \quad (4)$$

129 The forcing and dissipation, however small, are necessary for generating statistically stationary
 130 KE spectra in the DNS. To generate a -3 spectral slope, forcing was applied at the large scale:
 131 $f(t)$ was chosen to be an independent white-noise process for each 2D wavevector whose scalar
 132 wavenumber k falls in the narrow band ($\pm 10\%$) around $k = 20$. The dissipation d was a highly
 133 scale-selective hyperviscosity $d \sim -\Delta^6 \theta$.

134 It is worth noting that equation (4) would also be the vorticity form of the incompressible 2D-NS
 135 equations

$$\frac{\partial \mathbf{u}}{\partial t} + (\mathbf{u} \cdot \nabla) \mathbf{u} = -\nabla p + f(x, t) + \nu \Delta \mathbf{u}, \quad \nabla \cdot \mathbf{u} = 0 \quad (5)$$

136 if d were chosen to be $d = \nu \Delta \theta$, $\nu > 0$. We would have liked to run these DNS on the 2D-NS
 137 equations which will be discussed in Section 4, but the build-up of KE at the smallest scales as
 138 a numerical artefact was so strong that we had to either increase ν – which would substantially
 139 shorten the inertial range and thus reduce the reliability of our conclusions – or choose a more
 140 scale-selective dissipation. We opted for the latter.

141 We performed five pairs of identical-twin runs on equation (4) by varying the random seed that
 142 generated the pre-perturbation (original) initial condition. Within each pair, notably, the realisa-
 143 tions of the large-scale stochastic forcing $f(t)$ in the control and perturbed runs were identical.
 144 The model was pseudo-spectral with a truncation wavenumber of $k_t = 512$, in which the $J(\psi, \theta)$
 145 term was computed in the physical domain via a pair of Fast Fourier Transforms with the spectral
 146 de-aliasing filter proposed by Hou and Li (2007). The original initial condition for each of the
 147 five cases was an already-developed homogeneous and (approximately) isotropic turbulence with

148 a clean logarithmically corrected -3 spectrum in the inertial range (Figure 3), which has been
 149 shown to be a more accurate description of the large-scale-forced 2D turbulent spectrum for finite
 150 inertial ranges (Bowman 1996).

151 The perturbations were introduced spectrally at each of the 2D wavevectors \mathbf{k} for a specified
 152 value of $k_p = |\mathbf{k}|$. A random phase shift independently drawn from a uniform distribution was
 153 applied on a pre-determined part $\gamma \in [0, 1]$ of the spectral coefficients $\hat{\psi}(\mathbf{k})$ and thus $\hat{\theta}(\mathbf{k})$, where
 154 the hat indicates Fourier coefficients. It can be shown that $\gamma(k_p)$ and $\mathbb{E}(E_e(k_p))$, the expected value
 155 of the one-dimensional error KE spectral density at wavenumber k_p , are related by $\mathbb{E}(E_e(k_p)) =$
 156 $2\gamma^2 E(k_p)$, where $E(\cdot)$ is the one-dimensional KE spectral density of the background flow. By
 157 specifying the relative error $\frac{\mathbb{E}(E_e(k_p))}{E(k_p)}$, we could work out γ and thus generate the perturbation
 158 fields, to which we added the original initial conditions to obtain the perturbed initial conditions.

159 Since our truncation wavenumber $k_t = 512$ corresponds to $K = 9$ of Lorenz's paper, there would
 160 only be 8 values of $t_K - t_{K+1}$, among which only 4 or 5 would be in the inertial range. It would be
 161 inaccurate to determine β from such a few data points, so we have transformed Lorenz's argument
 162 to incorporate information from all wavenumbers k , not only from the scale K as a collection of
 163 wavenumbers.

164 To transform the argument, recall that $t_K \sim 2^{-\beta K}$ when $\beta > 0$. Since $k \sim 2^K$ and both t_K and T
 165 represent saturation times, we may write $T \sim k^{-\beta}$ and conclude that the T should vary with k as a
 166 power-law if Lorenz's results hold. The argument will break down when β becomes zero, that is,
 167 when the threshold for infinite predictability is reached.

168 In this study, the perturbations were introduced at $k_p = 256$. The saturation threshold was chosen
 169 to be 1.315 times the KE spectral density of the control flow, or equivalently 0.6575 times the
 170 maximum permissible error energy, in accordance with Lorenz (1969) (we applied sensitivity tests
 171 and found that the results are largely insensitive to the saturation threshold). Figures 4 and 5 show

172 respectively the evolution of the error KE spectrum, and the saturation times T across different
173 wavenumbers k which fit the $T \sim k^{-\beta}$ relationship for $\beta = 0.24$, averaged over the five cases.
174 (The five cases exhibited very similar qualitative behaviour, showing that our results are robust
175 to initial conditions, hence justifying the use of averaging to obtain smoother results.) Based on
176 the transformed version of Lorenz’s argument, our result also suggests finite predictability for a
177 (logarithmically corrected) -3 spectrum, this time with greater confidence as β is further away
178 from zero.

179 **4. Aspects from PDE theory: the incompressible 2D Navier-Stokes equations**

180 Although one may argue that the β found in the DNS (Section 3(b)) confirmed our earlier result
181 of finite predictability with Lorenz’s model (Section 3(a)), the non-trivial difference in the values
182 of β raises a concern that Lorenz’s argument may be over-simplified, particularly in respect of the
183 implied extrapolation of equation (3) to an infinitesimally small scale and the assumed linear p - β
184 relationship.

185 A very different approach to the problem of finite or infinite predictability is via use of the more
186 rigorous mathematical theory of partial differential equations (PDEs). The incompressible 2D-
187 NS equations (5), where we shall drop the word ‘incompressible’ for the remainder of the paper,
188 are always useful as a pedagogical first step towards understanding and modelling the motion of
189 real fluid flows in the atmosphere. As such, the analytical properties of the 2D-NS problem have
190 been extensively studied. We are however unaware of anyone taking this approach to address
191 predictability until recently.

193 Unlike their three-dimensional counterpart whose regularity problem remains open, the initial-
 194 value problem for the 2D-NS equations on the torus (i.e. a doubly periodic domain) has been
 195 proven to be well-posed, by which we mean the existence of a unique solution that depends con-
 196 tinuously on the initial conditions. Proofs of its well-posedness, for both strong and weak solutions
 197 respectively, can be found in the book by Robinson (2001). In the present paper we shall use his
 198 proof for weak solutions to demonstrate that the 2D-NS system is infinitely predictable. To set
 199 the context, a summary of the uniqueness proof is provided below. Interested readers may refer to
 200 Robinson's book for a full proof.

201 First of all, the 2D-NS equations (5) are cast in the form of an ordinary differential equation in
 202 an appropriate function space depending on an arbitrary, fixed positive time T . An equation for
 203 the error velocity field $w = u - v$ of two solutions u and v is formulated, and its inner product with
 204 w itself is taken to obtain an equation for the time-evolution of the error energy $\frac{1}{2}\|w\|^2$, where
 205 $\|\cdot\|$ is the L^2 norm on the torus. This equation contains a term which can be bounded above by
 206 Ladyzhenskaya's inequalities (Robinson 2001) specific to the 2D-NS equations. After some work
 207 one uses Grönwall's inequality to show that

$$\|w(t)\|^2 \leq \exp\left(\int_0^t \frac{M}{\nu} \|\nabla u(s)\|^2 ds\right) \|w(0)\|^2, \quad t \in [0, T],$$

208 where M is a positive constant provided by Ladyzhenskaya's inequalities. Uniqueness follows by
 209 setting $w(0) = 0$. One can also show the continuous dependence on initial conditions, since

$$\|w(t)\| \leq \sqrt{\exp\left(\int_0^T \frac{M}{\nu} \|\nabla u(s)\|^2 ds\right)} \|w(0)\| =: L(T) \|w(0)\|, \quad t \in [0, T], \quad (6)$$

210 i.e. errors are Lipschitz in time.

211 As an immediate corollary to inequality (6), the 2D-NS system is infinitely predictable (Palmer
 212 et al. 2014). Indeed, if a prediction is defined to lose its skill when $\|w(t)\| > \varepsilon$, then for any given

213 time $T \in \mathbb{R}^+$, the prediction is skilful for at least up to T when the initial error $\|w(0)\|$ can be made
 214 sufficiently small, that is, smaller than $\frac{\varepsilon}{L(T)}$.

215 It is important to note that in the present Section the KE spectral slope plays no role in deter-
 216 mining the finiteness or infiniteness of predictability of the 2D-NS equations. The above argument
 217 applies to 2D-NS systems of any spectral slope.

218 5. Reconciling the contradiction with Lorenz

219 At first glance, our result of infinite predictability derived in Section 4 seems to contradict
 220 Lorenz's result in Section 2 for any $p < 3$. However, we have not discussed the role of the KE
 221 spectral slope in $L(T)$ which, as we will see in the following, reconciles the conflict.

222 Central to our argument is the inequality (6) presented above. For simplicity, suppose the real
 223 system has only one inertial range of slope $-p$ (without any logarithmic correction) in its KE
 224 spectrum so that $|\hat{u}(k)|^2 \sim k^{-p}$ (note the change of notation: the hat now represents Fourier coeffi-
 225 cients in the space of one-dimensional wavenumbers k) between its large-scale cutoff wavenumber
 226 k_1 and small-scale cutoff wavenumber k_2 . Then

$$\|\nabla u_s\|^2 = \int_0^\infty k^2 |\hat{u}_s|^2 dk = \int_0^{k_1} k^2 |\hat{u}_s|^2 dk + A_0 \int_{k_1}^{k_2} k^{2-p} dk + \int_{k_2}^\infty k^2 |\hat{u}_s|^2 dk \quad (A_0 \text{ constant}), \quad (7)$$

227 where the subscript s distinguishes the system itself from a model for the system which we will
 228 denote with subscript m . The three terms on the right-hand-side of equation (7) represent contri-
 229 butions from the large scale, the inertial range and the viscous range respectively. Compared to
 230 the first two terms, the term representing the viscous range is assumed to be small. In particular,
 231 the integrand is assumed to decay rapidly enough so that $\|\nabla u_s\|^2$ remains finite (this is in fact part
 232 of the definition of the function space to which u_s belongs).

233 Now, suppose the model truncates at wavenumber $k_t \ll k_2$ and numerical dissipation kicks in at
 234 wavenumber $k_0 \in (k_1, k_t)$. For the model,

$$\|\nabla u_m\|^2 = \int_0^{k_t} k^2 |\hat{u}_m|^2 dk = \int_0^{k_1} k^2 |\hat{u}_m|^2 dk + A_0 \int_{k_1}^{k_0} k^{2-p} dk + \int_{k_0}^{k_t} k^2 |\hat{u}_m|^2 dk. \quad (8)$$

235 Again, we may neglect the contribution from the viscous range, so that

$$\|\nabla u_m\|^2 \sim \int_0^{k_1} k^2 |\hat{u}_m|^2 dk + A_0 \int_{k_1}^{k_0} k^{2-p} dk. \quad (9)$$

236 Because $k_0, k_t \ll k_2$, the second integral in relation (9) with $p < 3$ appears to diverge as the res-
 237 olution (k_0, k_t) increases. Combining this with inequality (6), $L(T)$ – until k_2 is reached – grows
 238 exponentially with k_0 , leading to a breakdown of the Lipschitz-continuous dependence on initial
 239 conditions in inequality (6). To keep the error $\|w(t)\|$ under control, the initial error $\|w(0)\|$ would
 240 have to decrease exponentially, but decreasing the scale of the initial error without changing its
 241 magnitude relative to the background KE spectral density (Lorenz’s thought experiment) would
 242 only give a polynomial decrease. The corollary of infinite predictability therefore fails to hold.
 243 Hence the range of predictability is finite in practice, even though the system is infinitely pre-
 244 dictable, because infinite predictability cannot be achieved without making the model resolution
 245 so high that its effective resolution k_0 (and the scale of the initial error) falls within the viscous
 246 range of the real system, let alone the large-scale error has to be constrained to zero (Durrant and
 247 Gingrich 2014).

248 This concept, known as ‘asymptotic ill-posedness’, was put forward by Palmer et al. (2014)
 249 as they argued that whether the three-dimensional Navier-Stokes system is well-posed is practi-
 250 cally irrelevant to the well-established theory of finite predictability. We have now extended the
 251 discussion to the 2D-NS system and given a mathematical basis to the concept in our context.

252 When $p > 3$, the second integral in relation (9) does not appear to diverge as $k_0 \rightarrow k_2$. This means
 253 one may indeed approximate $\|\nabla u_s\|^2$ by the $\|\nabla u_m\|^2$ in relation (9) with a sufficiently large value

254 of k_0 . So would $L(T)$ of inequality (6) be approximated without regard to the model resolution,
 255 making it possible for $\|w(t)\| \leq \varepsilon$ by making $\|w(0)\|$ small enough in scale and thus achieving
 256 infinite predictability.

257 So far our argument for the cases $p < 3$ and $p > 3$ are in harmony with Lorenz's result in
 258 Section 2. For the borderline case $p = 3$, our argument suggests practically finite predictability,
 259 since $\|\nabla u_m\|^2 \sim \text{constant} + \int_{k_1}^{k_0} k^{-1} dk = \text{constant} + \log \frac{k_0}{k_1}$ which appears to diverge as $k_0 \rightarrow k_2$.
 260 This disagrees with Lorenz. Even with the logarithmic correction

$$|\hat{u}(k)|^2 \sim k^{-3} \left[\log \left(\frac{k}{k_r} \right) \right]^{-\frac{1}{3}} \quad (k_r > 0 \text{ constant}),$$

261 or more generally

$$|\hat{u}(k)|^2 \sim k^{-3} \left[A_1 \log \left(\frac{k}{k_r} \right) + A_2 \right]^{-\frac{1}{3}} \quad (A_1, A_2, k_r > 0 \text{ constants}),$$

262 to the -3 spectrum (Bowman 1996), an easy calculation along the previous lines still suggests that
 263 the range of predictability is practically finite. As such, we are unable to explain the disagreement
 264 and we leave the problem open.

265 For models and systems with multiple inertial ranges, only the range immediately before viscous
 266 effects become important pertains to our argument concerning the large- k_0 behaviour. This applies
 267 to the real atmosphere where $p = \frac{5}{3}$ (Nastrom and Gage 1985). Since k_t for atmospheric models
 268 is smaller than k_2 by 'at least seven or eight orders of magnitude' (Palmer et al. 2014), the crucial
 269 assumption to our discussion ($k_t \ll k_2$) is satisfied and we conclude that atmospheric predictability
 270 is indeed practically finite.

271 6. Conclusions

272 Half a century on since Lorenz's pioneering argument of finite atmospheric predictability, we
 273 revisited his original argument by (i) re-running his simplified model of the 2D barotropic vorticity

274 equation, (ii) directly simulating the full model and (iii) comparing his conclusions with the well-
275 posedness of the 2D-NS equations as proven by Ladyzhenskaya.

276 Although his main conclusion – that atmospheric predictability is inherently finite because the
277 KE spectral slope is shallower than -3 – has now become an ‘accepted part of the canon of dynam-
278 ical meteorology’ (Rotunno and Snyder 2008), the details behind the conclusion were re-assessed.
279 The linearity assumption between the spectral slope $-p$ and β fails in his own simplified model
280 (Sections 2 and 3(a)) although we were unable to provide a simple, non-technical explanation. We
281 also saw a substantially different β in the DNS (Section 3(b)) than in Lorenz’s model, which may
282 be an indication that his model is inadequate in simulating the error growth. In both cases, nev-
283 ertheless, the hypothesis of infinite predictability ($\beta = 0$) for $p = 3$ based on linear extrapolation
284 was refuted.

285 The 2D-NS equations that closely relates to the 2D barotropic vorticity equation were used
286 to address the predictability problem from a more rigorous perspective. The forced-dissipative
287 system was shown to be infinitely predictable regardless of the spectral slope (Section 4). However,
288 we found that $p = 3$ serves as a cutoff between *practically* finite and infinite predictability by
289 noting how quickly the initial error has to be brought down with increasing resolution in order
290 to maintain the bound for the error at future times (Section 5). This echoes Lorenz’s original
291 conclusions except the borderline case $p = 3$ itself, in which case our result of finite predictability
292 agrees with our own computations of Lorenz’s model and the DNS.

293 Until recently, KE spectra in global weather forecast models had only resolved the synoptic-
294 scale -3 range. As model resolutions start to extend into the $-\frac{5}{3}$ range, the strong constraints
295 on the range of predictability envisaged by Lorenz will become relevant. However, the limits on
296 predictability arising from initial errors on the large scales will also limit predictability in practice

297 (Durran and Gingrich 2014), and the interplay between the two could be an interesting area to
298 explore.

299 By providing another approach to attacking the problem of predictability (via the analytic the-
300 ory of the 2D-NS equations), we look forward to similar results on more atmospherically relevant
301 PDEs such as the surface quasi-geostrophic equations (Held et al. 1995), and a more active contri-
302 bution from mathematicians on this topic.

303 *Acknowledgments.* Tsz Yan Leung is supported through a PhD scholarship awarded by the En-
304 gineering and Physical Sciences Research Council grant EP/L016613/1 ‘EPSRC Centre for Doc-
305 toral Training in the Mathematics of Planet Earth at Imperial College London and the University of
306 Reading’, with additional funding support from the European Research Council Advanced Grant
307 ‘Understanding the Atmospheric Circulation Response to Climate Change’ (ACRCC), Project
308 339390, under Theodore G. Shepherd as the Principal Investigator. The authors thank Richard
309 Scott for providing his code for modification for the numerical simulation in Section 3(b).

310 APPENDIX A

311 **Motivating the concept *range of predictability***

312 Standard theory in dynamical systems dictates that the dynamics of the error ε can be completely
313 described by the time t and the initial error ε_0 , so that $\varepsilon = \varepsilon(t, \varepsilon_0)$. Suppose now that the skill S
314 of a forecast can be quantified by a continuously decreasing function of some norm $\|\cdot\|$ (such as
315 the kinetic energy) of the error. In such a case, we can write $S = S(\|\varepsilon\|) = S(\varepsilon) = S(t, \varepsilon_0)$. If
316 we further assume that the error norm increases with t , we can infer that $S(t, \varepsilon_0)$ is monotonically
317 decreasing in time. We acknowledge that the assumption cannot be rigorously defended in the
318 context of atmospheric predictions, since it is typically observed in an average sense only.

319 Perhaps a first question to the understanding of predictability can be formulated as follows: how
 320 long does it take for an initial error ε_0 to grow so that a prediction loses its skill (defined by $S < \alpha$
 321 where α is a threshold of skill, and typically achieved in fluid flows by saturation of the error
 322 kinetic energy spectrum at specified scales)? The answer \tilde{T} , known as the range of predictability,
 323 is the solution to $S(t, \varepsilon_0) = \alpha$ for the specified ε_0 . The monotonicity assumption of S guarantees
 324 the uniqueness of the solution \tilde{T} .

325 By formulating this question for different initial error fields we can regard \tilde{T} as a function of
 326 ε_0 . It is clear from the very definition of deterministic systems that $\varepsilon_0 = 0$ implies $\tilde{T}(\varepsilon_0) = \infty$.
 327 However, it is not quite obvious as to whether \tilde{T} could be made arbitrarily large by reducing $\|\varepsilon_0\|$ to
 328 anything positive below a threshold, or equivalently whether the equality $\liminf_{\|\varepsilon_0\| \rightarrow 0} \tilde{T}(\varepsilon_0) = \infty$
 329 holds, because \tilde{T} may behave irregularly at small $\|\varepsilon_0\|$ – or at least appear to.

330 To see the equivalence, we unwrap the statement $\liminf_{\|\varepsilon_0\| \rightarrow 0} \tilde{T}(\varepsilon_0) = \infty$ to get

$$\liminf_{\|\varepsilon_0\| \rightarrow 0} \tilde{T}(\varepsilon_0) = \infty$$

$$\Leftrightarrow \forall R \in \mathbb{R}, \liminf_{\|\varepsilon_0\| \rightarrow 0} \tilde{T}(\varepsilon_0) \geq R$$

$$\Leftrightarrow \forall R \in \mathbb{R}, \sup_{\varepsilon' > 0} \inf_{\|\varepsilon_0\| \in (0, \varepsilon')} \tilde{T}(\varepsilon_0) \geq R$$

$$\Leftrightarrow \forall R \in \mathbb{R}, \exists \varepsilon' > 0 \text{ such that } \inf_{\|\varepsilon_0\| \in (0, \varepsilon')} \tilde{T}(\varepsilon_0) \geq R$$

$$\Leftrightarrow \tilde{T} \text{ could be made arbitrarily large by reducing } \|\varepsilon_0\| \text{ to anything positive below a threshold.}$$

331 With this in mind, a system is said to have an *infinite range of predictability*, or be *infinitely*
 332 *predictable*, if the range of predictability could be made arbitrarily large by reducing the initial
 333 error to a small yet positive value. Systems that fail to satisfy such a condition are referred to as
 334 *finitely predictable*.

APPENDIX B

Some details regarding the computation of the matrix C

The integrations were performed using `scipy.integrate.nquad` on Python which returned a warning message ‘IntegrationWarning: Extremely bad integrand behavior occurs at some points of the integration interval’ about the integrand’s singular behaviour, even if the integration domain were confined to the support of the integrand so that resources were not wasted in integrating zero regions. The warning disappeared by applying a change of coordinates (from logarithmic to Cartesian) in the integrand and accordingly the integration limits, which sped up the wall-clock time of the computation by a factor of about 9 as well. The entries of C computed by these two methods differ by no more than 0.0025%. Based on these observations, we are confident that our computations are accurate.

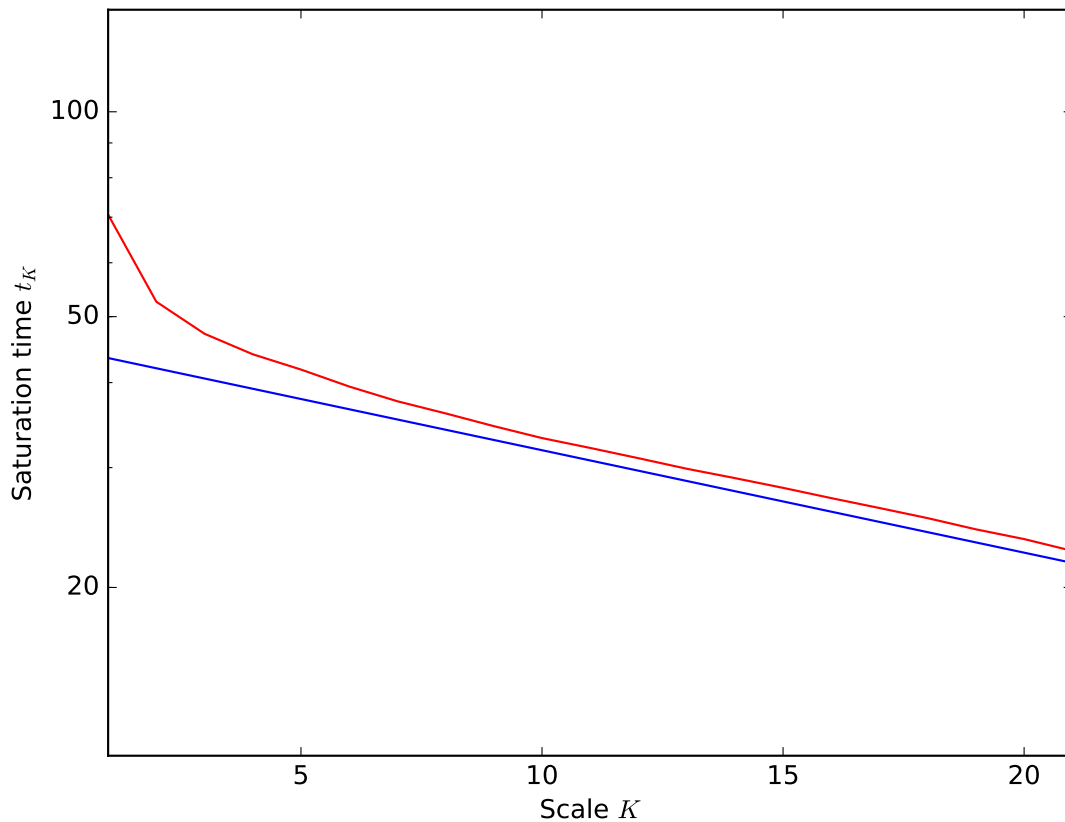
References

- Bowman, J. C., 1996: On inertial-range scaling laws. *J. Fluid Mech.*, **306**, 167–181, doi:10.1017/S0022112096001279.
- Durran, D. R., and M. Gingrich, 2014: Atmospheric predictability: why butterflies are not of practical importance. *J. Atmos. Sci.*, **71**, 2476–2488, doi:10.1175/JAS-D-14-0007.1.
- Held, I. M., R. T. Pierrehumbert, S. T. Garner, and K. L. Swanson, 1995: Surface quasi-geostrophic dynamics. *J. Fluid Mech.*, **282**, 1–20, doi:10.1017/S0022112095000012.
- Hou, T. Y., and R. Li, 2007: Computing nearly singular solutions using pseudo-spectral methods. *Journal of Computational Physics*, **226**, 379–397, doi:10.1016/j.jcp.2007.04.014.
- Lorenz, E. N., 1969: The predictability of a flow which possesses many scales of motion. *Tellus*, **21**, 289–307, doi:10.3402/tellusa.v21i3.10086.

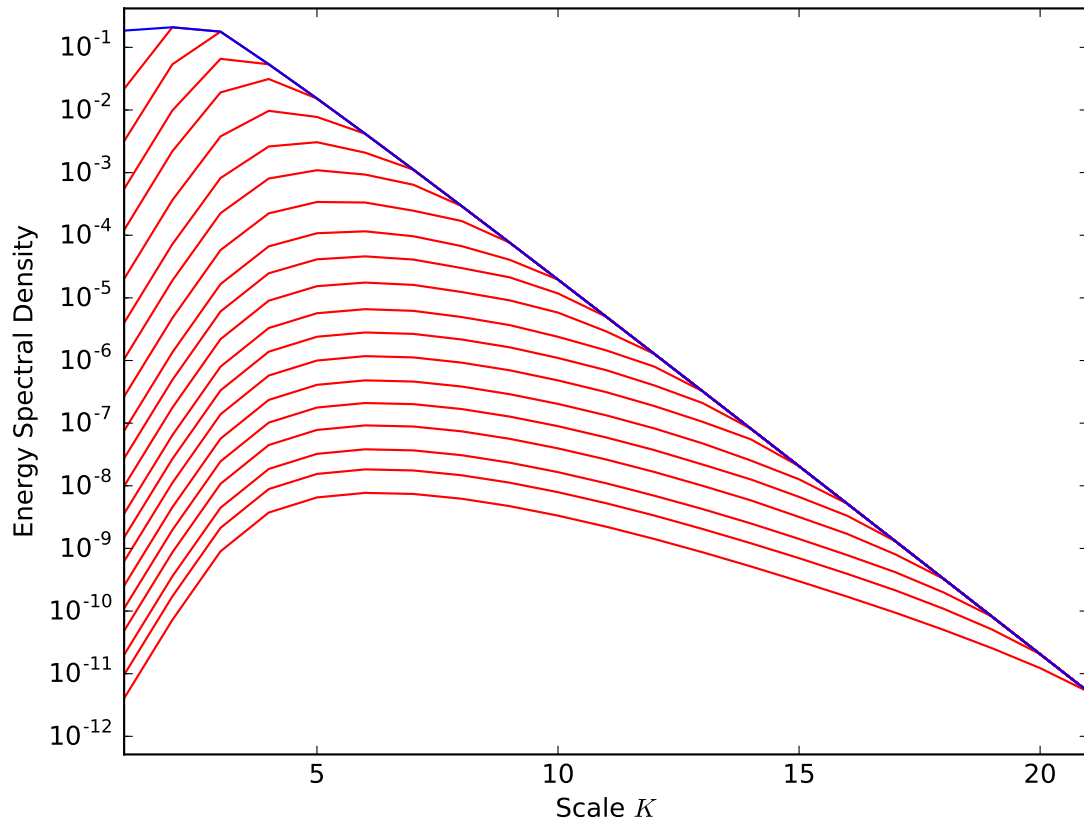
- 357 Nastrom, G. D., and K. S. Gage, 1985: A climatology of atmospheric wavenumber spectra of
358 wind and temperature observed by commercial aircraft. *J. Atmos. Sci.*, **42**, 950–960, doi:10.
359 1175/1520-0469(1985)042<0950:ACOAWS>2.0.CO;2.
- 360 Palmer, T. N., A. Döring, and G. Seregin, 2014: The real butterfly effect. *Nonlinearity*, **27**, R123–
361 R141, doi:10.1088/0951-7715/27/9/R123.
- 362 Robinson, J. C., 2001: *Infinite-Dimensional Dynamical Systems: An Introduction to Dissipative*
363 *Parabolic PDEs and the Theory of Global Attractors*. Cambridge University Press, 234–257 pp.
- 364 Rotunno, R., and C. Snyder, 2008: A generalization of Lorenz’s model for the predictability of
365 flows with many scales of motion. *J. Atmos. Sci.*, **65**, 1063–1076, doi:10.1175/2007JAS2449.1.
- 366 Sun, Y. Q., and F. Zhang, 2016: Intrinsic versus practical limits of atmospheric predictabil-
367 ity and the significance of the butterfly effect. *J. Atmos. Sci.*, **73**, 1419–1438, doi:10.1175/
368 JAS-D-15-0142.1.

LIST OF FIGURES

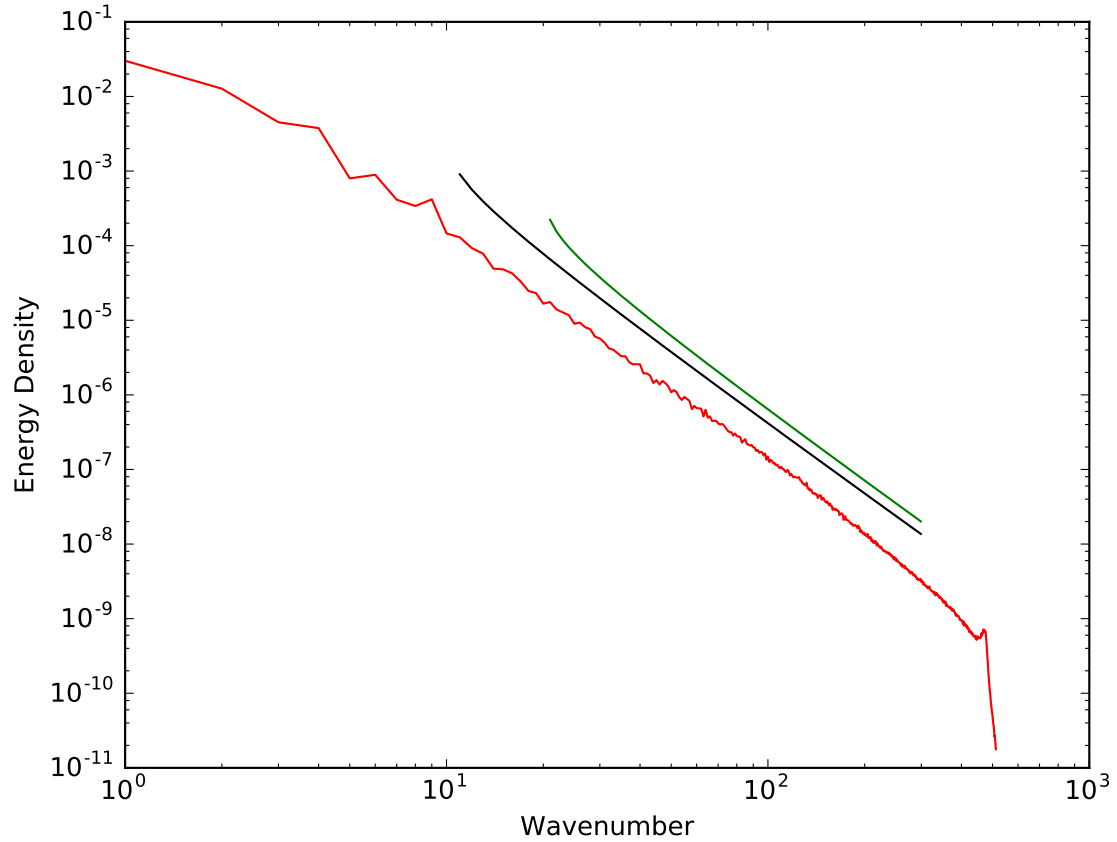
369		
370	Fig. 1.	Saturation times of various scales in the Lorenz (1969) model (red), with a -3 -slope background KE spectrum as in Rotunno and Snyder (2008). The initial condition for this run is of a tiny magnitude at the second smallest of the 21 scales available. The blue curve shows a line of fit with $\beta = 0.05$ 21
371		
372		
373		
374	Fig. 2.	The evolution of error KE spectra (red, from bottom to top) and the background spectrum (blue) for the same model run as Figure 1. 22
375		
376	Fig. 3.	KE spectrum (averaged over the five cases) of the initial condition (red), and logarithmically corrected -3 reference spectra $E(k) \sim k^{-3} \left[\log \left(\frac{k}{k_r} \right) \right]^{-\frac{1}{3}}$ ($k_r = 10$ in black, $k_r = 20$ in green), where $E(\cdot)$ is the one-dimensional KE spectral density. 23
377		
378		
379	Fig. 4.	Evolution of the error KE spectrum (magenta and blue, bottom to top) for an initial perturbation (blue dot) at $k_p = 256$. The magenta curves are for $t = 0.3, 0.6, \dots, 2.7$ and the blue curves are for $t = 3, 6, \dots, 66$. The background KE spectra at $t = 0, 3, 6, \dots, 66$, scaled by a factor of 2, are shown in red (top to bottom), with the reference spectra in black and green as in Figure 3. The spectra are averaged over the five cases. 24
380		
381		
382		
383		
384	Fig. 5.	Saturation times T at different wavenumbers k (red) for an initial error at wavenumber $k_0 = 256$, averaged over the five cases. The black curve shows a line of fit with $\beta = 0.24$ 25
385		



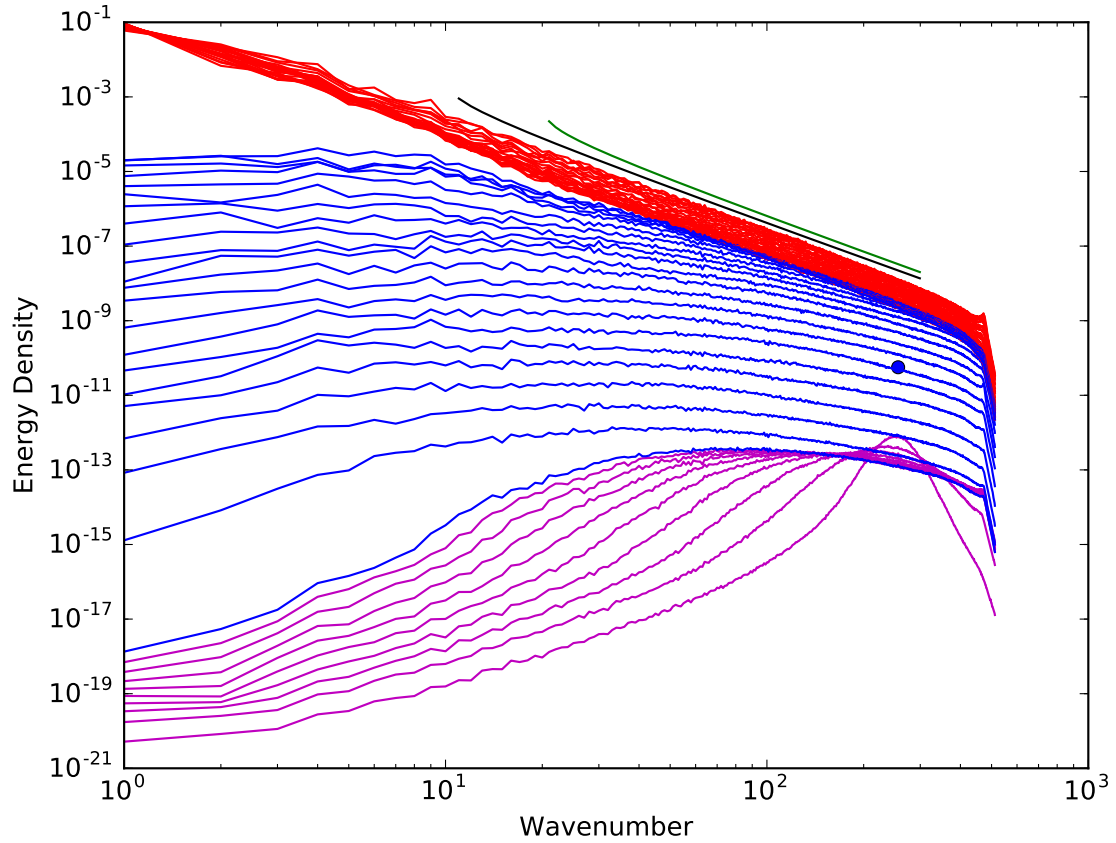
386 FIG. 1. Saturation times of various scales in the Lorenz (1969) model (red), with a -3 -slope background KE
 387 spectrum as in Rotunno and Snyder (2008). The initial condition for this run is of a tiny magnitude at the second
 388 smallest of the 21 scales available. The blue curve shows a line of fit with $\beta = 0.05$.



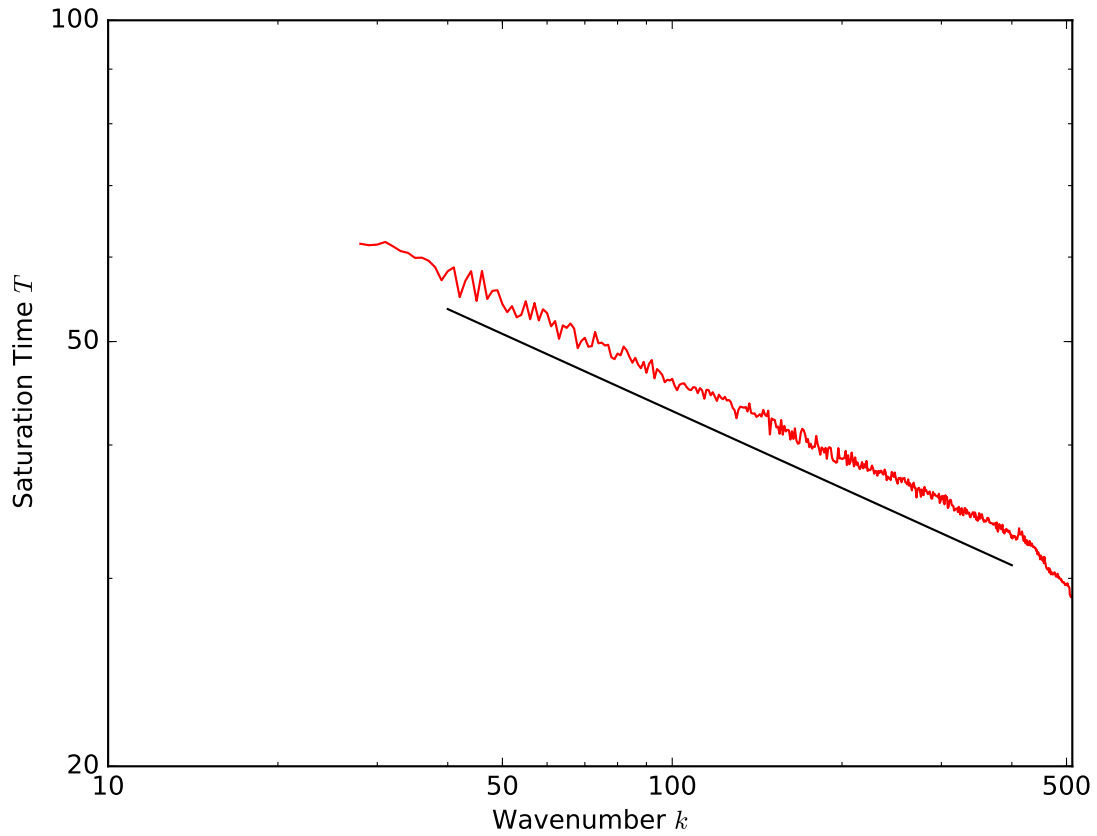
389 FIG. 2. The evolution of error KE spectra (red, from bottom to top) and the background spectrum (blue) for
390 the same model run as Figure 1.



391 FIG. 3. KE spectrum (averaged over the five cases) of the initial condition (red), and logarithmically corrected
 392 -3 reference spectra $E(k) \sim k^{-3} \left[\log \left(\frac{k}{k_r} \right) \right]^{-\frac{1}{3}}$ ($k_r = 10$ in black, $k_r = 20$ in green), where $E(\cdot)$ is the one-
 393 dimensional KE spectral density.



394 FIG. 4. Evolution of the error KE spectrum (magenta and blue, bottom to top) for an initial perturbation (blue
 395 dot) at $k_p = 256$. The magenta curves are for $t = 0.3, 0.6, \dots, 2.7$ and the blue curves are for $t = 3, 6, \dots, 66$. The
 396 background KE spectra at $t = 0, 3, 6, \dots, 66$, scaled by a factor of 2, are shown in red (top to bottom), with the
 397 reference spectra in black and green as in Figure 3. The spectra are averaged over the five cases.



398 FIG. 5. Saturation times T at different wavenumbers k (red) for an initial error at wavenumber $k_0 = 256$,
399 averaged over the five cases. The black curve shows a line of fit with $\beta = 0.24$.